



**HAL**  
open science

## Measurement of subwoofers with the field separation method: comparison of p- p and p-v formulations

Manuel Melon, Christophe Langrenne, Alexandre Garcia

### ► To cite this version:

Manuel Melon, Christophe Langrenne, Alexandre Garcia. Measurement of subwoofers with the field separation method: comparison of p- p and p-v formulations. Acoustics 2012, Apr 2012, Nantes, France. hal-00810930

**HAL Id: hal-00810930**

**<https://hal.science/hal-00810930v1>**

Submitted on 23 Apr 2012

**HAL** is a multi-disciplinary open access archive for the deposit and dissemination of scientific research documents, whether they are published or not. The documents may come from teaching and research institutions in France or abroad, or from public or private research centers.

L'archive ouverte pluridisciplinaire **HAL**, est destinée au dépôt et à la diffusion de documents scientifiques de niveau recherche, publiés ou non, émanant des établissements d'enseignement et de recherche français ou étrangers, des laboratoires publics ou privés.



# ACOUSTICS 2012

## Measurement of subwoofers with the field separation method: comparison of p- p and p-v formulations

M. Melon, C. Langrenne and A. Garcia

Conservatoire National des Arts et Métiers, 292 rue Saint-Martin 75141 Paris Cedex 03  
manuel.melon@cnam.fr

Measurement of very low frequency sources is rather difficult to perform because very few testing rooms remain anechoic in the 10-100 Hz frequency range. To overcome this problem, the field separation method has been proposed a few years ago. This technique consists in measuring two acoustic quantities on a closed surface surrounding the tested source. To take advantages of spherical harmonic functions, the measurement surface should be spherical. The acoustic quantities can either be acoustic pressure measured on two concentric (half-) spheres or pressure and velocity measured on a (half-) sphere. Then, by using spherical harmonic expansions, contribution from the subwoofer is separated from reflections on the walls of the testing rooms to recover half or free space conditions. This paper focuses on the choice of the measured data set. Simulations are performed using p-p and p-v data approaches. The effect of microphone spacing for the double pressure layer formulation will be investigated. Finally, measurement results obtained on a subwoofer will be shown to highlight simulation results.

## 1 Introduction

Measurement of low frequency sources like subwoofers is not an easy task. In this frequency range, very few dead rooms remain anechoic. Different solutions were proposed for the assessment of the frequency response: outdoor measurements, windowing of measured signals, pressure measurements in the near-field (or even inside the box) of the tested source. However, these solutions have drawbacks and cannot always be used. An alternative method consists in measuring two acoustic fields on closed surfaces surrounding the tested source. Knowing these two data sets allows the separation of the outgoing field coming from the subwoofer from the incoming field radiated by the other sources or reflected by walls of the testing room. This approach has been first proposed by Weinreich *et al.* [1] for the measurement of a violin. It has later been applied to the measurement of subwoofers in a semi anechoic room [2] or in a usual room [3]. For the results reported in these two last papers, the separation process was performed with pressure and velocity data (p-v approach). However, separation can also be calculated with a set of two pressure fields measured on two concentric spheres (p-p approach). This paper focuses on these two possibilities and tries to evaluate which one is the most efficient in the 10 – 400 Hz frequency range.

## 2 Theory

A brief summary of the p-p and p-v approaches will be given here, for a more detailed description please consult reference [4]. Consider three concentric spheres of respective radii  $r_1$  to  $r_3$ , where  $r_2 = \frac{r_1+r_3}{2}$ . The chosen time dependence is given by  $e^{j\omega t}$  and will be omitted throughout the paper.

### 2.1 p-v approach

Acoustic pressure and velocity fields are measured on the sphere of radius  $r_2$  and then expanded on spherical harmonic functions:

$$p(r_2, \theta, \phi) = \sum_{n=0}^{\infty} \sum_{m=-n}^n \alpha_{nm} Y_n^m(\theta, \phi) \quad (1)$$

$$v(r_2, \theta, \phi) = \sum_{n=0}^{\infty} \sum_{m=-n}^n \beta_{nm} Y_n^m(\theta, \phi) \quad (2)$$

where  $\theta$  is the colatitude,  $\phi$  is the longitude, and  $Y_n^m$  are the normalized spherical harmonic functions. The  $\alpha_{nm}$  and  $\beta_{nm}$  coefficients can be obtained from measurement data by matrix inversion or by expansion using orthonormal properties

of  $Y_n^m$ . This formulation can be rewritten in terms of outgoing and standing waves:

$$p(a_2, \theta, \phi) = \sum_{n=0}^{\infty} \sum_{m=-n}^n [a_{mn} h_n^{(2)}(ka_2) + b_{mn} j_n(ka_2)] Y_n^m(\theta, \phi) \quad (3)$$

$$v(a_2, \theta, \phi) = \frac{-j}{\rho_0 c} \sum_{n=0}^{\infty} \sum_{m=-n}^n [a_{mn} h_n^{\prime(2)}(ka_2) + b_{mn} j_n^{\prime}(ka_2)] Y_n^m(\theta, \phi) \quad (4)$$

The spherical Bessel functions  $j_n$  represent the standing wave field while the spherical Hankel functions  $h_n^{(2)}$  represent the outgoing field. The  $a_{mn}$  coefficients are given by:

$$a_{mn} = jk^2 a_2^2 [j \rho_0 c \beta_{mn} j_n(ka_2) - \alpha_{mn} j_n^{\prime}(ka_2)], \quad (5)$$

which allow the calculation of the outgoing field. This latter represents the field that would have been radiated under free field conditions.

### 2.2 p-p approach

In the case where acoustic pressure is measured on the spheres of radius  $r_1$  and  $r_3$ , expansions of the two fields on spherical harmonic functions are given by:

$$p(a_1, \theta, \phi) = \sum_{n=0}^{\infty} \sum_{m=-n}^n \gamma_{nm} Y_n^m(\theta, \phi) \quad (6)$$

$$p(a_3, \theta, \phi) = \sum_{n=0}^{\infty} \sum_{m=-n}^n \delta_{nm} Y_n^m(\theta, \phi) \quad (7)$$

Pressure fields can also be written in terms of outgoing and standing waves:

$$p(a_1, \theta, \phi) = \sum_{n=0}^{\infty} \sum_{m=-n}^n (c_{mn} h_n^{(2)}(ka_1) + d_{mn} j_n(ka_1)) Y_n^m(\theta, \phi) \quad (8)$$

$$p(a_3, \theta, \phi) = \sum_{n=0}^{\infty} \sum_{m=-n}^n (c_{mn} h_n^{(2)}(ka_3) + d_{mn} j_n(ka_3)) Y_n^m(\theta, \phi) \quad (9)$$

The processing of the outgoing field can be performed by using:

$$c_{mn} = \frac{j_n(ka_1) \delta_{mn} - j_n(ka_3) \gamma_{mn}}{\Delta}, \quad (10)$$

with:  $\Delta = j_n(ka_1) h_n^{(2)}(ka_2) - j_n(ka_2) h_n^{(2)}(ka_1)$ . Please note that  $\Delta$  can be null, however when dealing with the measurement of subwoofer, the first zero is out the frequency band of interest. For instance, with  $a_1 = 0.6$  m and  $a_3 = 0.7$  m, the first zero is obtained for  $f > 1700$  Hz

When the spacing  $d = a_3 - a_1$  between the two spheres is

small compared to the wavelength,  $\Delta$  can be expanded in Taylor series. By using the Wronskian relation for spherical Bessel functions, one can show that  $\Delta \approx \frac{jd}{ka_1^2}$  thus giving an simplified solution for  $c_{mn}$ :

$$c_{mn} = \frac{ka_1^2}{jd} [j_n(ka_1)\delta_{mn} - j_n(ka_3)\gamma_{mn}], \quad (11)$$

### 2.3 Practical implementation

To make the measurements easier, the tested subwoofer is placed on the rigid ground of the testing room. Then, measured data are collected on concentric half-spheres. Please note that in this case, the separation process will only remove reflections from walls and ceiling thus giving half-space conditions. The mathematical implication of this measurement geometry is that expansions can be performed only on even spherical harmonics to respect the problem symmetry (thus only even values of  $m + n$  are used).

Another practical consideration is the finite number of measurement points which limits the expansion maximum order  $N$ . When using even spherical harmonic functions, each hemisphere should be discretized with at least  $\sum_{i=0}^N (i + 1)$  points.

Note that it is possible to compute the p-v approach from double layer pressure measurements if  $a_3 - a_1$  is much smaller than the wavelength. In this case, the mean pressure is used and approximation of Euler's equation by finite difference is performed to calculate velocity.

## 3 Simulations

Tests are performed using half-spheres with 36 probe positions. The placing of the measurement points is shown on Figure 1. With an optimal placing of the 36 measurement points, expansions can be performed up to order  $N = 7$ . With the regular mesh used here having more than required points near the pole,  $N$  decreases to 5.

The following radii will be used :  $a_1 = 0.6$  or  $0.625$  m,  $a_2 = 0.65$  m and  $a_3 = 0.7$  or  $0.675$  m. This configuration gives a maximum studying frequency  $f_m = \frac{cN}{2\pi a_3} \approx 388$  Hz .

A first test has been processed with a first monopole lo-

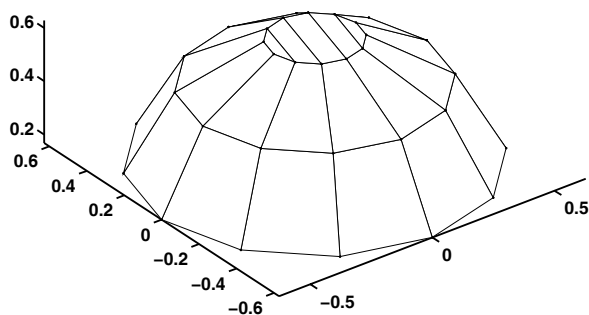


Figure 1: Placing of the probes on a measurement surface.

cated inside the half-spheres at coordinates (0.1 m, 0 m, 0.07

m) while the second monopole lies outside the measurement surfaces at coordinates (1 m, 0 m, 1 m). The separation process is applied to the simulated data using four different algorithms:

- The p-v implementation (pv) based on pressure and velocity fields simulated for radius  $a_2$  (Eq. 5).
- The p-p implementation (pp) based on pressure fields simulated for radii  $a_1$  and  $a_3$  (Eq. 10).
- The Taylor series approximation of the p-p implementation (ppa) using (Eq. 11).
- The finite difference implementation (pva), for which pressure and velocity fields are processed from pressure measurements on radii  $a_1$  and  $a_3$  by using first order approximations.

A cumulative error criteria  $E$  is calculated between the estimated pressure obtained from separation  $p_i^e(a_2, \theta, \phi)$  and the theoretical pressure  $p_i^t(a_2, \theta, \phi)$  on the measurement points of the median half-sphere:

$$E = \sqrt{\frac{\sum_{i=1}^{36} |p_i^e(a_2, \theta, \phi) - p_i^t(a_2, \theta, \phi)|^2}{\sum_{i=1}^{36} |p_i^t(a_2, \theta, \phi)|^2}}. \quad (12)$$

Results are plotted in Figure 2. One can see that, when pressure and velocities are accurately known, there is no difference between the pp and pv approaches, the two curves are superimposed.  $E$  is very low below  $f_m$  and increases sharply when approaching  $f_m$ . The error rate is slightly higher for pva due to the approximations on pressure and velocity on the median half-sphere.  $E$  is much larger for ppa, and surprisingly the curve does merge with pp values at very low frequency. This can be explained by the fact that spherical Hankel function grows very fast, thus first order approximation is not sufficient.

To study the effect of noise on the separation process, ran-

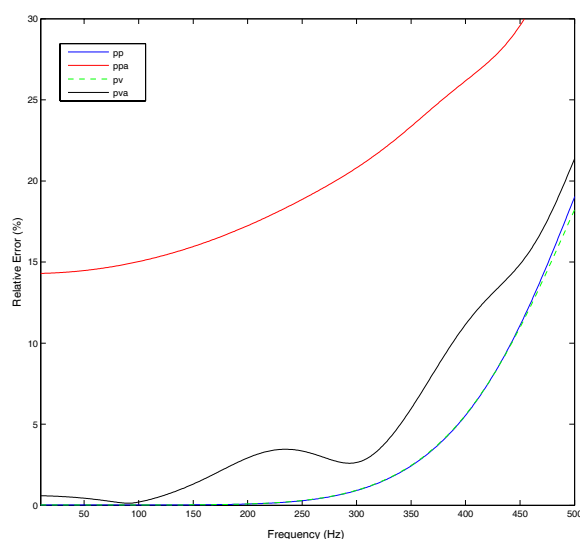


Figure 2: Relative errors for the four separation algorithms for  $d = 10$  cm

dom errors have been added to the simulated data on the measurement half-spheres. Amplitude has been blurred with

a noise of maximum amplitude equal to 7% of the maximum theoretical pressure while normal distributed phase errors with a standard deviation of 0.1 degrees have been added to the simulated data. Results for 50 averaged acquisitions are shown in Figure 3. Error rate for the pv method shows a moderate increase compared to the previous case but remains below 1% up to 300 Hz. At low frequencies error rates for pp and pva are very close (about 2 – 3 %), at higher frequencies  $E_{pp}$  merges with  $E_{pv}$ .

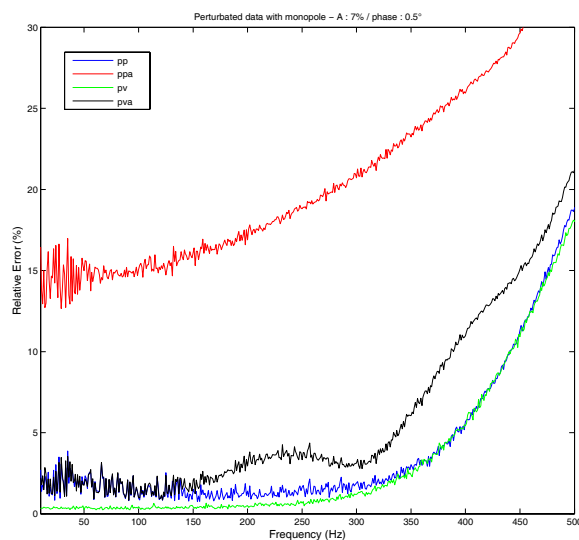


Figure 3: Relative errors for the four separation algorithms with added noise for  $d = 10$  cm

Simulations without and with added noise have also been processed for  $d = 5$  cm. Results are shown in Figures 4 and 5. One can see that pp, pv and pva have very similar error rates when no noise is applied do the simulated data. With a small microphone spacing, finite approximations of pva are very close to actual pressures and velocities on the median half-sphere. Error rate for ppa remains high even in this favourable case. When noise is added to the amplitude and phase of the measured data (maximum values of 10 % of the maximum pressure and 0.5 degrees),  $E_{pp}$  and  $E_{pva}$  are very close in the tested frequency band. The pv method have the lowest error rate  $< 2$  % up to 300 Hz.

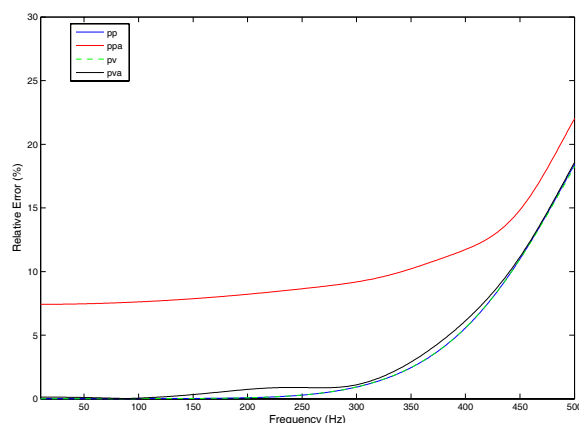


Figure 4: Relative errors for the four separation algorithms for  $d = 5$  cm.

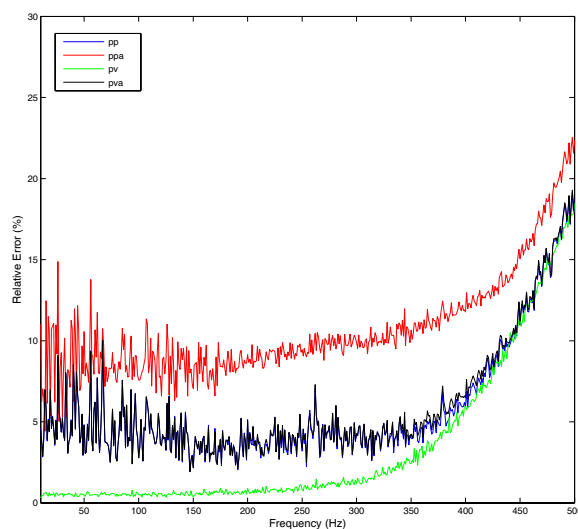


Figure 5: Relative errors for the four separation algorithms with added noise for  $d = 5$  cm.

## 4 Measurements

A closed box subwoofer has been built with thin walls to highlight the impact of the enclosure vibrations. The box is a cube with edge length of 0.395 m and is made of medium density fiberboard (MDF) wood. A Peerless 269 SWR 51 XLS loudspeaker is mounted on the box. The loudspeaker is driven by a band limited white noise (10 Hz-500 Hz) test signal. The test signal is not filtered, however, an additional  $4.8 \Omega$  series resistance is inserted between the amplifier and the loudspeaker.

The tested subwoofer is put on the rigid ground of a semi-anechoic chamber. A p-p probe, calibrated in amplitude and phase, is moved on two hemispherical surfaces by an automated positioning system. The distance between the two microphones is 10 cm. The geometry of the measurement system is shown in Figure 6.

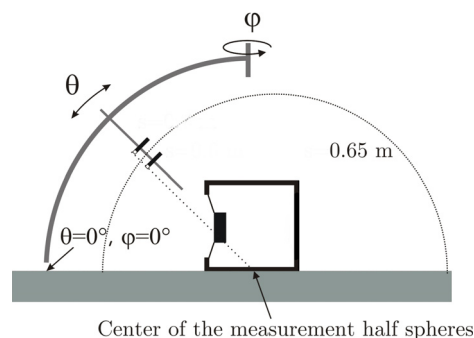


Figure 6: Geometry of the measurement set-up.

The enclosure and membrane normal velocities have also been measured using a scanning Laser Doppler Vibrometer (Polytec OFV 056 / OFV 3001 S) at each point of a  $15 \times 15$  grid on each of the five accessible subwoofer faces. After velocities have been measured, a BEM modelling of the subwoofer has been performed. The mesh is made with 1009 points decomposed onto quadrangular elements with 4

nodes. The pressure field is then computed using normal velocities and a Green function which takes the rigid ground into account. The values obtained with the BEM modelling will be used as reference values.

A comparison of the measured pressure and of the pressure computed by BEM is given in Figure 7 for a point in front of the membrane and in Figure 8 for a point at the back of the subwoofer. The discrepancy between the measured and BEM curves is high at low frequency where the semi-anechoic room is no longer anechoic. But there are also differences above 200 Hz that can reach 3 dB due to the presence of the positioning system. Differences between BEM and measured data are larger at the back of the subwoofer because the probe is more distant from the membrane.

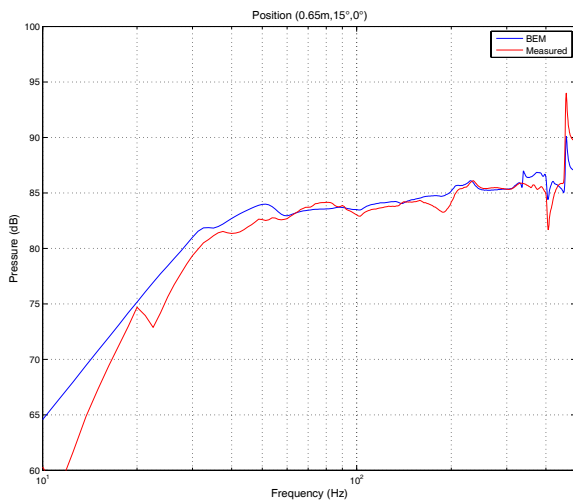


Figure 7: Measured and BEM pressures in front of the membrane.

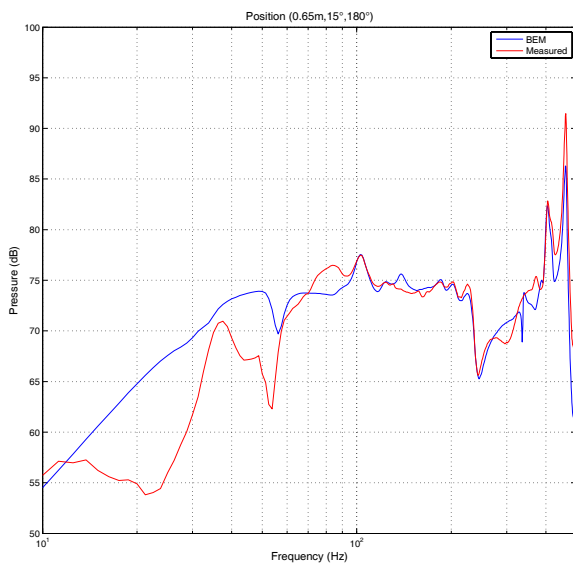


Figure 8: Measured and BEM pressures at the back of the subwoofer

The field separation method is applied to the measured pressure fields using pp, ppa and pva algorithms (no p-v probe was available at the time of measurements). Results are plot-

ted in figures 9 for a point in front of the membrane and in Figure 10 for a point at the back of the subwoofer. As seen in the simulation section, the ppa processing does not give accurate results. The results obtained here follow this trend. For the pp and pva processing, curves obtained from the separation process are generally closer to the BEM curve than the measured one. The pp and pva methods give the same results up to 250 Hz. Between 250 Hz and 500 Hz, the two curves deviates from a maximum of 1 dB. Although, neither of these two methods seems to be always closer to the BEM curve.

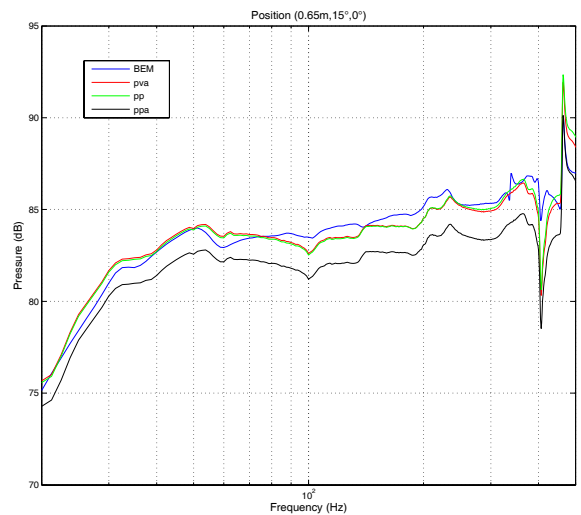


Figure 9: FSM and BEM pressures in front of the membrane.

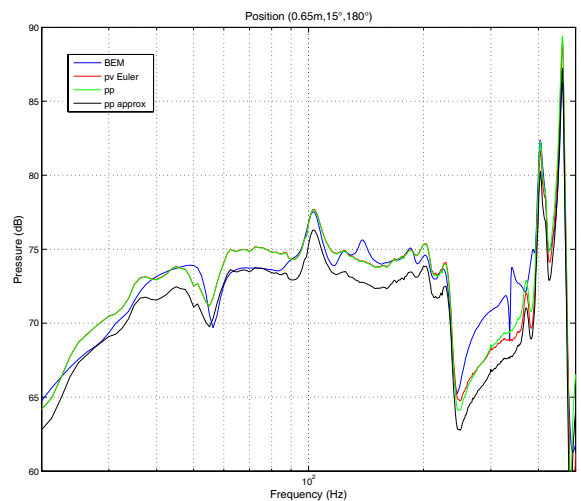


Figure 10: FSM and BEM pressures at the back of the subwoofer

## 5 Summary

In this paper, four different implementations of the field separation method have been tested to measure the frequency response of a closed box subwoofer. The pressure field radiated by the subwoofer was mainly blurred by reflections on

the walls of the semi-anechoic room below 180 Hz and by scattering on the positioning system above 180 Hz. From the simulation and measurements reported here, one can draw the following conclusions.

- The ppa method should not be used. When using a very small microphone spacing, the error rate is strongly reduced however this configuration becomes very sensitive to measurement noise.
- The pv method always gives the better results especially when noise is added to the measurement data. In practice, this approach can be carried out with a Microflown probe. Future work should be conducted to evaluate the benefit of this configuration. A special attention should be given to the calibration of the p-v probe and to the sensitivity to noise of pressure and velocity in actual conditions.
- The pp method gives the same results as the pv method when data are almost free from errors but is more sensitive to noise especially for low values of  $a_3 - a_1$ . This result can be explained by the fact that when reducing microphone spacing, pressure fields on the two half spheres become very similar thus degrading the calculation of the  $c_{mn}$  coefficients.
- The pva method is not as accurate as the pv and pp methods when no noise is added to the data. Although, in presence of random errors, the error rate can approach values obtained with the pp method depending on the microphone spacing and on the noise level.

Please note that these conclusions were drawn at low frequencies. At higher frequencies, the pva method which relies on first order approximations of acoustic pressure and velocity would be less efficient.

## References

- [1] G. Weinreich and E. B. Arnold, Method for measuring acoustic radiation fields, *J. Acoust. Soc. Am.* **68**(5), 404–411 (1980).
- [2] M. Melon, C. Langrenne, D. Rousseau, and P. Herzog, “Comparison of four subwoofer measurement techniques,” *J. Audio. Eng. Soc.* **55**(12), 1077–91 (2007).
- [3] M. Melon, C. Langrenne, P. Herzog, and A. Garcia, “Evaluation of a method for the measurement of subwoofers in usual rooms,” *J. Acoust. Soc. Am.* **127**(1), 256–263 (2010).
- [4] E. G. Williams, *Fourier Acoustics*, Academic Press, London (1999).